On the geometrically nonlinear vibration of a piezo-flexomagnetic nanotube

Mohammad Malikan[1], Victor A. Eremeyev[1,2*]

[1]Department of Mechanics of Materials and Structures, Faculty of Civil and Environmental Engineering, Gdansk University of Technology, 80-233, Gdansk, Poland

[2]Don State Technical University, Gagarina sq., 1, Rostov on Don 344000, Russia

*Corresponding author: victor.eremeev@pg.edu.pl, eremeyev.victor@gmail.com

Acknowledgements

V.A.E acknowledges the support of the Government of the Russian Federation (contract No. 14.Z50.31.0046).

Abstract

In order to describe the behavior of thin elements used in MEMS and NEMS, it is essential to study a nonlinear free vibration of nanotubes under complicated external fields such as magnetic environment. In this regard, the magnetic force applied to the conductive nanotube with piezo-flexomagnetic elastic wall is considered. By the inclusion of Euler-Bernoulli beam and using Hamilton's principle, the equations governing the system are extracted. More importantly, a principal effect existed in a nonlinear behavior such as axial inertia is thoroughly analyzed which is not commonly investigated. We then consider the effects of nanoscale size using the nonlocal theory of strain gradient (NSGT). Hereafter, the frequencies are solved as semi-analytical solutions on the basis of Rayleigh-Ritz method. The piezo-flexomagnetic nanotube (PF-NT) is calculated with different boundary conditions. In order to validate, the results attained from the present solution have been compared with those available in the open literature. We realized that the nonlinear frequency analysis is so significant when a nanotube has fewer degrees of freedom at both ends, and its length is long.

Keywords: Nonlinear vibration; Piezo-flexomagnetic nanotubes; Axial inertia; NSGT; Rayleigh-Ritz method

1. Introduction

Nano-electro-mechanical systems (NEMS) are the technology of very small nanometer-sized machines. NEMS is a step ahead of micro-electro-mechanical systems (MEMS) and usually encompasses a combination of transistors (electric), sensors and motors (mechanical). Due to its very small size, NEMS is expected to have a major impact on large sections of science and technology and eventually replace MEMS [1].

Contemporarily, a discovered and explored phenomenon known in the elements of electro-mechanical coupling with taking magnetic effect is flexomagneticity. Uniform strain makes magnetic polarization, and the response is reflected by piezomagneticity. This occurrence exists only in dielectrics with non-centrosymmetric structures. A lot of studies showed that a non-zero magnetic field can be induced by the inclusion of non-uniform strains. Flexomagnetic (FM) effect defines this type of coupling of an induced magnetic field and distribution of the non-uniform strain [2-4]. Flexomagneticity in comparison with piezomagneticity, demonstrates the coupling features of induced magnetic polarization and strain gradient. Flexomagneticity becomes a remarkable and overcoming influence when the material size is scaled down to nanoscale, although this effect is meager and negligibly small on macro scale. Therefore, a further conceptual understanding of the FM on NEMS is necessary.

In a general understanding through FM, during polarization in the material, strain gradient induces magnetic field and magnetic field gradient induces the strain. The former is named as the direct impact and the later one as the converse effect. The FM already is on the novel threshold of its research.

To predict the mechanical response of NEMS, a great deal can be observed done on piezomagneticity during the contemporary decade [5-20], though the literature on FM is much less developed, see, e.g., [21-23]. The analysis of nanomaterials containing FM was commenced by Sidhardh and Ray [21] by surveying a cantilever nanoscale size piezomagnetic Euler-Bernoulli beam subjected to transverse static loading. The surface elasticity was developed on the model. Moreover, both converse and direct magnetic

effects were discussed. Zhang et al. [22] extended FM studies to asses bending analysis of a small scale piezomagnetic Euler-Bernoulli beam under several conditions of boundaries. They investigated both reverse and direct FM. Malikan and Eremeyev [23] modeled the linear dynamic conditions for a nanotube involving FM and evaluated scale effect on the basis of stress-driven nonlocal elasticity. The size-dependency behavior of FM was corroborated by their findings as well.

As far as very limited studies are found on FM, one can acquisition many opportunities to account for such the effect. This research intends to expand the FM on a nanosize Euler-Bernoulli beam. More importantly, the vibration problem is described with respect to nonlinear strains of Lagrangian based von Kármán assumptions [24-33]. It is worth to mention that the effect of axial inertia may become important in parts of vibrating machines. So, this effect is estimated as well. Plus, size-dependence is modeled with exerting nonlocal strain gradient theory (NSGT). In view of nonlinear partial differential equations, the analytical solution methods are unable to give a solution. By virtue of this, numerical solution techniques should come in hand, such as differential quadrature method (DQM) [34, 35], finite difference method (FDM) [36], finite element method (FEM) [37, 38], mesh free method [39], dynamic relaxation method (DRM) [40], Homotopy method [41], etc. These techniques take a long time to give the numerical results due to their massive computations. Amidst solution approaches, semi-analytical techniques require lower time to grant the numerical outcomes. The Rayleigh-Ritz technique is a one that based on a few convergence rate solves the equations with shorter formulation. On the basis of very general assumptions, the Rayleigh-Ritz shows its advantage. In terms of the approximation features, this method produces optimal solutions. Thus, the solution process is here accomplished by means of Rayleigh-Ritz technique. Thereby, a validation section is provided to render the correctness of the formulation. Thereupon, numerical results are reported by creating different pictorial figures for momentous parameters.

2. Mathematical model

Let us consider a typical nanotube of length L, of thickness h and of diameter d. Figure 1 shows a schematic image of the considered structure [42].

In what follows we consider the Euler-Bernoulli beam model for the considered nanotube. Moreover, we restrict ourselves to in-plane deformations. So, the middle neutral beam line coincides with the *x*-axis whereas *z*-axes relates to the transverse direction. The corresponding Cartesian displacements are denoted as u_1 and u_3, respectively, see [43-46] for detail. The axial and transverse displacements of the middle neutral line are denoted by *u* and *w*, respectively. So, the kinematical relations are given by

$$u_1(x,z,t) = u(x,t) - z\frac{\partial w(x,t)}{\partial x} \tag{1}$$

$$u_3(x,z,t) = w(x,t) \tag{2}$$

Based on the von Kármán nonlinear strains, in the Lagrangian strain formula, the nonlinear term related to *u* is adequately small and can be ignorable. Accordingly, the nonlinear components of the axial strain and its gradient are calculated as

$$\varepsilon_{xx} = \frac{\partial u}{\partial x} - z\frac{\partial^2 w}{\partial x^2} + \frac{1}{2}\left(\frac{\partial w}{\partial x}\right)^2 \tag{3}$$

$$\eta_{xxz} = \frac{\partial \varepsilon_{xx}}{\partial z} = -\frac{\partial^2 w}{\partial x^2} \tag{4}$$

where η_{xxz} means gradient of the elastic strain. Following [21, 22] the one-dimensional stress-strain magneto-mechanical relations are prepared as

$$\sigma_{xx} = C_{11}\varepsilon_{xx} - q_{31}H_z \tag{5}$$

$$\xi_{xxz} = g_{31}\eta_{xxz} - f_{31}H_z \tag{6}$$

$$B_z = a_{33}H_z + q_{31}\varepsilon_{xx} + f_{31}\eta_{xxz} \tag{7}$$

where σ_{xx} and ξ_{xxz} are the stress and hyper stress, B_z and H_z are the magnetic flux and the magnetic field, respectively, and material parameters are introduced. In particular, $C_{11} = C_{1111}$ is the elastic modulus, $f_{31} = f_{3311}$ denotes the component of the fourth-order flexomagnetic coefficients tensor, a_{33} represents the component of the second-order magnetic permeability tensor, $q_{31} = q_{311}$ depicts the component of the third-order piezomagnetic tensor, and $g_{31} = g_{311311}$ is the component the sixth-order gradient elasticity tensor.

In order to precisely extract the particularized equation of piezo-flexomagnetic type nanotubes (PF-NTs), the variational formulation can be expanded adequately on the base of Hamilton's principle as

$$\int_{t_1}^{t_2}\left(\delta K-\delta U+\delta W\right)dt=0 \tag{8}$$

in which δ denotes the symbol of variation. In (8), the first variation of the total internal of the beam is equal to zero, and the other factors are the kinetic and strain energies (K and U) and the created work by outer forces (δW).

The first variation of the strain energy can be written in an integral form according to magneto-mechanical coupling as

$$\delta U=\int_V\left(\sigma_{xx}\delta\varepsilon_{xx}+\xi_{xxz}\delta\eta_{xxz}-B_z\delta H_z\right)dV \tag{9}$$

Using assumed 1D kinematics and integrating by parts, we can transform (9) in to a sum

$$\delta U=\delta\Pi_{U_1}^{Mech}+\delta\Pi_{U_1}^{Mag}+\delta\Pi_{U_2}^{Mech}+\delta\Pi_{U_2}^{Mag}$$

where

$$\delta\Pi_{U_1}^{Mech}=-\int_0^L\left(\frac{\partial N_x}{\partial x}\delta u+\frac{\partial^2 M_x}{\partial x^2}\delta w+\frac{\partial}{\partial x}\left(N_x\frac{\partial w}{\partial x}\right)\delta w+\frac{\partial^2 T_{xxz}}{\partial x^2}\delta w\right)dx \tag{10a}$$

$$\delta\Pi_{U_1}^{Mag}=-\int_0^L\int_{-h/2}^{h/2}\frac{\partial B_z}{\partial z}\delta\Psi dzdx \tag{10b}$$

$$\delta\Pi_{U_2}^{Mech}=\left(N_x\delta u-M_x\frac{\partial\delta w}{\partial x}-T_{xxz}\frac{\partial\delta w}{\partial x}+N_x\frac{\partial w}{\partial x}\delta w+\frac{\partial M_x}{\partial x}\delta w+\frac{\partial T_{xxz}}{\partial x}\delta w\right)\Bigg|_0^L \tag{11a}$$

$$\delta\Pi_{U_2}^{Mag}=\int_0^L\left(B_z\delta\Psi\right)\Big|_{-h/2}^{h/2}dx \tag{11b}$$

and we also have introduced normal axial force, moment and hyperstress as follows

$$N_x=\int_{-h/2}^{h/2}\sigma_{xx}dz \tag{12}$$

$$M_x=\int_{-h/2}^{h/2}\sigma_{xx}zdz \tag{13}$$

$$T_{xxz} = \int_{-h/2}^{h/2} \xi_{xxz} dz \tag{14}$$

In our case the work of external forces has the functional

$$W = -\frac{1}{2}\int_0^L N_x^0 \left(\frac{\partial w}{\partial x}\right)^2 dx \tag{15}$$

which first variation has the form

$$\delta W = -\int_0^L N_x^0 \left(\frac{\partial \delta w}{\partial x}\frac{\partial w}{\partial x}\right) dx \tag{16}$$

where N_x^0 presents the initial in-plane axial force.

In addition in (11b) we introduced the magnetic potential Ψ. The relationship between magnetic potential and magnetic field component can be given by

$$H_z + \frac{\partial \Psi}{\partial z} = 0 \tag{17}$$

By accounting a reverse flexomagnetic state for a closed circuit, one can attribute the following conditions

$$\Psi\left(+\frac{h}{2}\right) = \psi, \ \Psi\left(-\frac{h}{2}\right) = 0 \tag{18a-b}$$

in which the potential on the top surface as a result of the magnetic field is symbolized by ψ. The change of the magnetic potential along the thickness of the nanotube and then the component of the magnetic field can be feasible by the use of Eqs. (7), (10b), (11b), (17), and (18) [21, 22]

$$\Psi = -\frac{q_{31}}{2a_{33}}\left(z^2 - \frac{h^2}{4}\right)\frac{\partial^2 w}{\partial x^2} + \frac{\psi}{h}\left(z + \frac{h}{2}\right) \tag{19}$$

$$H_z = z\frac{q_{31}}{a_{33}}\frac{\partial^2 w}{\partial x^2} - \frac{\psi}{h} \tag{20}$$

Thereafter, Eqs. (5)-(7) on the basis of Eqs. (19) and (20) can be expanded as

$$B_z = q_{31}\left[\frac{\partial u}{\partial x} + \frac{1}{2}\left(\frac{\partial w}{\partial x}\right)^2\right] - f_{31}\frac{\partial^2 w}{\partial x^2} - \frac{a_{33}\psi}{h} \tag{21}$$

$$\xi_{xxz} = -\left(g_{31} + \frac{q_{31}f_{31}z}{a_{33}}\right)\frac{\partial^2 w}{\partial x^2} + \frac{f_{31}\psi}{h} \tag{22}$$

$$\sigma_{xx} = C_{11}\left[\frac{\partial u}{\partial x} + \frac{1}{2}\left(\frac{\partial w}{\partial x}\right)^2\right] - z\left(C_{11} + \frac{q_{31}^2}{a_{33}}\right)\frac{\partial^2 w}{\partial x^2} + \frac{q_{31}\psi}{h} \tag{23}$$

which are magnetic induction, the component of higher-order moment stress tensor and the component of stress field, respectively.

Therefore, magneto-mechanical stress resultants (Eqs. (12)-(14)) can be re-written as

$$N_x = C_{11}A\left[\frac{\partial u}{\partial x} + \frac{1}{2}\left(\frac{\partial w}{\partial x}\right)^2\right] + q_{31}\psi \tag{24}$$

$$M_x = -I_z\left(C_{11} + \frac{q_{31}^2}{a_{33}}\right)\frac{\partial^2 w}{\partial x^2} \tag{25}$$

$$T_{xxz} = -g_{31}h\frac{\partial^2 w}{\partial x^2} + f_{31}\psi \tag{26}$$

where $I_z = \int_A z^2 dA$ is dedicated for area moment of inertia.

According to Eq. (24), axial stress resultant involves mechanical and magnetic parts. Thus, the magnetic axial stress resultant can be presented as

$$N^{Mag} = q_{31}\psi \tag{27}$$

where we suppose the above value as axial magnetic force acted on both ends of the nanotube (due to longitudinal magnetic field), hence

$$N_x^0 = N^{Mag} \tag{28}$$

The kinetic energy can be associated with the nanotube as follows

$$K = \frac{1}{2}\int\int_A \rho(z)\left[\left(\frac{\partial u_1}{\partial t}\right)^2 + \left(\frac{\partial u_3}{\partial t}\right)^2\right]dAdz \tag{29}$$

or with (1) and (2) as

$$K = \frac{1}{2}\int\int_A \rho(z)\left[\left(\frac{\partial u}{\partial t} - z\frac{\partial^2 w}{\partial x \partial t}\right)^2 + \left(\frac{\partial w}{\partial t}\right)^2\right]dAdz \tag{30}$$

Finally, the first variational schema of kinetic energy would be

$$\delta K = \int_A\left[-I_0\frac{\partial^2 u}{\partial t^2}\delta u + I_1\frac{\partial^3 w}{\partial x \partial t^2}\delta u - I_1\frac{\partial^3 u}{\partial x \partial t^2}\delta w + I_2\frac{\partial^4 w}{\partial x^2 \partial t^2}\delta w - I_0\frac{\partial^2 w}{\partial t^2}\delta w\right]dA \tag{31}$$

where $\left\{I_0, I_1, I_2 = \int_{-h/2}^{h/2} \rho(z)\left(1, z, z^2\right) dz\right\}$ is depicted for the mass moments of inertia.

The corresponding magneto-mechanical governing equations can be derived by imposing Eq. (8) as

$$\frac{\partial N_x}{\partial x} = I_0 \frac{\partial^2 u}{\partial t^2} - I_1 \frac{\partial^3 w}{\partial x \partial t^2} \tag{32}$$

$$\frac{\partial^2 M_x}{\partial x^2} + \frac{\partial^2 T_{xxz}}{\partial x^2} + \frac{\partial}{\partial x}\left(N_x \frac{\partial w}{\partial x}\right) = I_0 \frac{\partial^2 w}{\partial t^2} + I_1 \frac{\partial^3 u}{\partial x \partial t^2} - I_2 \frac{\partial^4 w}{\partial x^2 \partial t^2} \tag{33}$$

Due to their premier chemical, electrical and mechanical properties, nanostructured elements such as nanobeams, nanotubes, nanoshells, and nanosheets are customarily used as components in nano-electro-mechanical devices. Therefore, accurate prediction of the vibrational characteristics of nanostructures is essential for engineering and production design. On the other hand, classical mechanic theory cannot predict the size-effect at the nanoscale. At the nanoscale, size-effects became important and even dominated. Both the experimental results and the results of the molecular dynamics simulation show that the size-effect on the mechanical properties of materials is extraordinary and meaningful when the dimensions of these structures are scaled down. To tackle this problem, there can be found three methods proposed for analyzing nanostructures, namely atomic mechanics [47, 48], atomic-continuum mechanics (multiscale methods) [49, 50] and continuum mechanics [51]. However, the third method has a lower computational cost than the previous two methods. In this research, the theory of non-classical continuum mechanics is utilized. It should be noted that this theory itself is divided into several sub-theories. Some researchers have used couple stress theories to examine the effect of scale [52-57], others have employed Eringen's nonlocal theory [58-64], some have utilized the theory of first and second strain gradient elasticity [65-68], and some other researchers have exerted a combination of these theories. They have merged and incorporated more up-to-date theories, such as the nonlocal theory of strain gradient [69], or the stress-driven nonlocal elasticity theory [70, 71]. Some also have developed Eringen's nonlocal theory [72, 73]. In this study, the nonlocal theory of strain gradient is used, which may simulate more accurate the mechanical behavior of nanostructures in continuous models. The nature of this theory is based on two principles: first, stress at any point is a function of strain at the same point and also in all parts of the

body, which is known as the nonlocal section; and second, strain gradients in a material particle are substantial which this part is well-known as gradient section. Researchers in the field of nanomechanics of continuous models have significantly moved toward this theory in recent years and have benefited from it [74-82].

In this section, the nonlocal elasticity model of strain gradient for the PF-NT is expanded in a general form as follows [69, 83-85]:

$$\left(1-\mu\frac{\partial^2}{\partial x^2}\right)\sigma_{xx}^{NonLocal}=\left(1-l^2\frac{\partial^2}{\partial x^2}\right)\left\{C_{11}\left[\frac{\partial u}{\partial x}+\frac{1}{2}\left(\frac{\partial w}{\partial x}\right)^2\right]-z\left(C_{11}+\frac{q_{31}^2}{a_{33}}\right)\frac{\partial^2 w}{\partial x^2}+\frac{q_{31}\psi}{h}\right\} \quad (34)$$

where $l(nm)$ is the gradient parameter and $l>0$ establishes non-zero strain gradient into the model; and $\mu(nm^2)$ allocates nonlocality. Noted that $\mu(nm)^2=(e_0a)^2$ in which e_0 and a are two small scale factors that determine the nonlocal parameter. It is germane to note that both factors are dependent on the nature of the model and physical conditions and cannot be material constants [86, 87]. This means they are not a constant value for each material something like elasticity modulus.

The effect of small scale on the stress resultants can be implemented by plugging Eq. (34) to Eqs. (24)-(26) as

$$N_x-\mu\frac{\partial^2 N_x}{\partial x^2}=\left(1-l^2\frac{\partial^2}{\partial x^2}\right)\left\{C_{11}A\left[\frac{\partial u}{\partial x}+\frac{1}{2}\left(\frac{\partial w}{\partial x}\right)^2\right]+q_{31}\psi\right\} \quad (35)$$

$$M_x-\mu\frac{\partial^2 M_x}{\partial x^2}=\left(1-l^2\frac{\partial^2}{\partial x^2}\right)\left\{-I_z\left(C_{11}+\frac{q_{31}^2}{a_{33}}\right)\frac{\partial^2 w}{\partial x^2}\right\} \quad (36)$$

$$T_{xxz}-\mu\frac{\partial^2 T_{xxz}}{\partial x^2}=\left(1-l^2\frac{\partial^2}{\partial x^2}\right)\left\{-g_{31}h\frac{\partial^2 w}{\partial x^2}+f_{31}\psi\right\} \quad (37)$$

Note that due to lack of a third additional equation, the small scale effects for Eq. (37) are omitted. Eqs. (35) and (36) with respect to Eqs. (32) and (33) can be simplified as

$$\begin{aligned}N_x=&\mu\left(I_0\frac{\partial^3 u}{\partial x\partial t^2}-I_1\frac{\partial^4 w}{\partial x^2\partial t^2}\right)\\&+C_{11}A\left[\frac{\partial u}{\partial x}+\frac{1}{2}\left(\frac{\partial w}{\partial x}\right)^2-l^2\left(\frac{\partial^3 u}{\partial x^3}+\frac{\partial^2 w}{\partial x^2}\frac{\partial^2 w}{\partial x^2}+\frac{\partial w}{\partial x}\frac{\partial^3 w}{\partial x^3}\right)\right]+q_{31}\psi\end{aligned} \quad (38)$$

$$M_x = -\mu\left(\frac{\partial^2 T_{xxz}}{\partial x^2} - N_x^0\frac{\partial^2 w}{\partial x^2} - I_0\frac{\partial^2 w}{\partial t^2} - I_1\frac{\partial^3 u}{\partial x \partial t^2} + I_2\frac{\partial^4 w}{\partial x^2 \partial t^2}\right)$$
$$-I_z\left(C_{11} + \frac{q_{31}^2}{a_{33}}\right)\left(\frac{\partial^2 w}{\partial x^2} - l^2\frac{\partial^4 w}{\partial x^4}\right) \tag{39}$$

In this paper, we discuss PF-NT with reference to homogeneity in the material; therefore, I_1 will disappear.

In the case of a nonlinear conservative system, we can consider nonlinear oscillations as follows. First, let us note that in this case we have non-harmonic oscillations, that is $u(x,t) \neq v_1(x)\cos(\omega t)$, and $w(x,t) \neq v_2(x)\cos(\omega t)$ in general. Nevertheless, for conservative systems we have periodic solutions as

$$u(x,t) = v_1(x,t) = v_1(x,t+T) \tag{40}$$

$$w(x,t) = v_2(x,t) = v_2(x,t+T) \tag{41}$$

where T is a minimal period. We replace T using the relation $T = 2\pi/\omega$ in which ω is frequency. Moreover, v_1 and v_2 are the vibration amplitudes.

The following change of variable $\omega t \to \tau$ can be made. In this case, we get

$$\frac{\partial v_1}{\partial t} = \omega\frac{\partial v_1}{\partial \tau} \tag{42}$$

$$\frac{\partial v_2}{\partial t} = \omega\frac{\partial v_2}{\partial \tau} \tag{43}$$

Thus, strain and kinetic energies can be written in the framework of below

$$U = \frac{1}{2}\int_0^L \left\{\sigma_{xx}\left[\frac{\partial v_1}{\partial x} - z\frac{\partial^2 v_2}{\partial x^2} + \frac{1}{2}\left(\frac{\partial v_2}{\partial x}\right)^2\right]\right\}dx \tag{44}$$

$$K = \frac{1}{2}\int_0^L \left\{I_0\omega^2\left[\left(\frac{\partial v_1}{\partial \tau}\right)^2 + \left(\frac{\partial v_2}{\partial \tau}\right)^2\right] + I_2\omega^2\left(\frac{\partial^2 v_2}{\partial x \partial \tau}\right)^2\right\}dx \tag{45}$$

$$W = -\frac{1}{2}\int_0^L N_x^0\left(\frac{\partial v_2}{\partial x}\right)^2 dx \tag{46}$$

As approximate solutions we can use

$$v_1(x,\tau) = V_1(x)\cos\tau \tag{47}$$

$$v_2(x,\tau) = V_2(x)\cos\tau \tag{48}$$

Then integrating by time from the obtained equation over (0, 2π) will exclude the time from the equations.

Note that in the following the real part of frequency is considered only. Finally, putting Eqs. (37)-(39) into Eqs. (44)-(46), then connecting Eqs. (44)-(46) together ($K+U+W=0$) and imposing Hamiltonian gives the characteristic equation of frequency of the PF-NT which can be shortened and simplified as below

$$\left(\omega^2 M + K_1\right)\{X\} + \{X\} K_2 \{X\} = 0 \tag{49}$$

in which K_1, K_2, and M are coefficients related to stiffness and mass, respectively, and $X = \begin{Bmatrix} V_1 \\ V_2 \end{Bmatrix}$.

3. Rayleigh-Ritz approach

To catch a general solution for the aforesaid nonlinear equation (Eq. (49)), the analytical solutions are mostly incapable and restricted to get a solution. Moreover, numerical methods consume a large time to present a solution [88, 89]. On the other side, semi-analytical techniques, e.g., the Rayleigh-Ritz method presented its simplicity and speed of solving to compute the eigenvalue problems that existed in engineering problems [90-94]. This method in what follows will be indicated.

$$V_1(x) = \sum_{j=1}^{N} a_j \varphi_j(x) \tag{50a}$$

$$V_2(x) = \sum_{j=1}^{N} b_j \psi_j(x) \tag{50b}$$

in which N denotes a number of considered base elements and will determine the convergence to the exact solution, a_j and b_j are the unknown variables to be determined and, φ_j and ψ_j denote the basic mode shapes demonstrated as below

$$\varphi_j(x) = f_\varphi T_j(x) \tag{51a}$$

$$\psi_j(x) = f_\varphi T_j(x) \tag{51b}$$

where

$$f_{\varphi}=\left(\frac{x}{L}\right)^{\eta}\times\left(1-\frac{x}{L}\right)^{\xi} \tag{52}$$

in which η and ξ associates an exponent to convey various boundary conditions (BCs) as seen in Table 1. Here SS, CS, CC denote the simply supported – simply supported, clamped-simply supported, and clamped–clamped BCs, respectively. Other polynomial base function is defined as

$$T_j = x^{j-1} \tag{53}$$

The dedicated kinematic and nonlocal strain gradient constitutive boundary conditions can be expressed by Table 2 [95-98]

Herein, by means of the simple solution of the quadratic polynomial equation (Eq. (49)), the results of nonlinear frequency can be determined. The positive values are considered only.

4. Numerical results

4.1. Results' accreditation

In this subsection in order to validate the model and the proposed technique, Eq. (49) will be reduced to a simple case to receive the validation. To achieve the simple case, we avoid the strain gradient effect, piezomagnetic and FM properties of the problem; however, we take the nonlocality into account. To do this, on the basis of Rayleigh-Ritz formulation, the simple case can be converted into two subcases, namely nonlinear and linear parts as shown by Eq. (54) and (55). In addition to these, we also investigate the results of the Navier solution technique for this simple case as illustrated by Eq. (56). Furthermore, in order to identify the accuracy of the present Rayleigh-Ritz formulation, a reference is dedicated as [99] and the numerical comparison is tabulated by Table 3. It is to be noted that here N=5 as [93, 100].

- Rayleigh quotient based on the nonlinear strains and simple case:

$$\omega_{NL}^2=\frac{C_{11}I_z\int_0^L\left(\frac{\partial^2 V_2}{\partial x^2}\right)^2dx+C_{11}A\int_0^L\left[\frac{\partial V_1}{\partial x}+\frac{1}{2}\left(\frac{\partial V_2}{\partial x}\right)^2\right]^2dx}{\int_0^L\left[I_0{V_2}^2+I_2\left(\frac{\partial V_2}{\partial x}\right)^2-\mu\left(I_0V_2\frac{\partial^2 V_2}{\partial x^2}-I_2\left(\frac{\partial^2 V_2}{\partial x^2}\right)^2\right)\right]dx} \tag{54}$$

- Rayleigh quotient based on the linear strains and simple case:

$$\omega_L^2 = \frac{I_z C_{11} \int_0^L \left(\frac{\partial^2 v_2}{\partial x^2} \right)^2 dx}{\int_0^L \left[I_0 {v_2}^2 + I_2 \left(\frac{\partial v_2}{\partial x} \right)^2 - \mu \left(I_0 v_2 \frac{\partial^2 v_2}{\partial x^2} - I_2 \left(\frac{\partial^2 v_2}{\partial x^2} \right)^2 \right) \right] dx} \tag{55}$$

- Navier-type solution with linear strains and simple case:

$$\omega^2 = \frac{I_z C_{11} \left(\frac{\pi}{L} \right)^4}{\mu \left[I_0 \left(\frac{\pi}{L} \right)^2 + I_2 \left(\frac{\pi}{L} \right)^4 \right] + I_0 + I_2 \left(\frac{\pi}{L} \right)^2} \tag{56}$$

The tabular validation is regarding the growth of slenderness ratio (L/h), and nonlocal parameter (μ). Also, the following elasticity property; $E=1TPa$ is used, and the thickness is considered as $h=1nm$. Moreover, the frequencies are dimensionless using $\Omega = \omega L^2 \sqrt{\frac{\rho A}{EI}}$.

Clearly, the comparative results between outputs of Navier-type solution in the present paper and those attained by the literature present a completely acceptable correlation. On the other side, there cannot be observed any difference among the outputs of linear Rayleigh-Ritz method compared with the Navier cases even for higher values of nonlocal parameter as well as of slenderness ratio.

Elseway, the nonlinear frequencies are indicated by Table 4 by [101-103] and the ratio between nonlinear and linear instances are calculated. To indicate an approvement for the values of nonlinear frequency computed and obtained in this work, we consider SS edge conditions. Based on the demonstrated and tabulated results, the outcomes of present nonlinear analysis can be confirmed.

4.2. Discussion of the problem

Obviously, no one can find a frequency analysis of a PF-NT while geometrically nonlinearity is taken into account. To estimate the present problem, the existence

quantities in Table 5 are employed [21, 22]. Note that all the eigenfrequencies extracted in the section are respecting the first mode only.

To consider a NSGT case, both nonlocal and strain gradient parameters perform outstanding roles. In point of fact, the values of both factors determine the value of frequency. As far as it was mentioned before about depending of these factor's values on many situations, Thus, exploring among the literature to pick up a logical limit for both parameters can be a time-effective choice. For nonlocal parameter the 0.5 nm$<e_0a<$0.8 nm [90], and $0<e_0a\leq$2 nm [104, 105], were found and then can be applied. However, there was no reference for strain gradient parameter values. Therefore, a lower bound limit is chosen for the values.

4.2.1 The effect of nonlocal parameter

Figure 2 carries out the influence of the nonlocal parameter versus both linear and nonlinear analyses of eigenfrequency. It is visible that the nonlinear case demonstrates greater results. This may be due to the fact that physically the geometrically nonlinear analysis gives the material axial forces because of presence of tension in mid-surface. So, the frequency capability of material will be higher which will lead to higher frequencies. Moreover, the nonlinear analysis eliminates the strain as a result of rigid displacements in a large deflection study (Note that in our work the mean of rigid displacement is any movement without deformation). Thus, e.g., in a nonlinear bending analysis the deflections will be lesser compared to the linear case. In a nonlinear vibration problem, the mode shapes will be bigger and the material because of large deformations, can capture higher frequencies.

As seen by the figure, any incremental change in the amount of nonlocal parameter leads to a decrease in dimensionless frequency values. This effect and the decreasing trend are more apparent when the less flexible end condition is considered. In fact, the slope is steeper. The most obvious result of the figure is the lesser effect of nonlinear analysis against the linear one for simple supported–simple supported end conditions. Physically, it can be interpreted that when the type of boundary condition is more flexible, the displacements and deflections are further rigid. Therefore, the difference between results of nonlinear and linear states is smaller in such the boundaries. This means that the beam

has little stability and the material of the beam does not show significant resistance to large displacement, and therefore we do not see a substantial difference between nonlinear and linear frequencies in these cases. When the boundary condition has fewer degrees of freedom, the stretching effect more appears in the layers of thickness and large deformations are established more, which results in a noticeable difference in the results of nonlinear frequency versus linear in such the boundary conditions. Finally, as a last case in the figure, it can be said that the greatest frequencies are related to the boundary condition with the lowest degrees of freedom.

4.2.2 The effect of strain gradient parameter

One of the most important results of comparing nonlinear to linear frequency analysis in Figure 3 has been shown by changing the numerical values of the strain gradient parameter. In the figure, the range of the value of the strain gradient parameter is considered from zero to 2 nm for different boundary conditions. Returning to the figure, it is visible that increase of the values of the strain gradient parameter leads to augmenting the distance between nonlinear and linear frequency results. It may be how interpreted that when the numerical value of the strain gradient parameter increments, the hardening effect of the material enhances and the frequencies naturally become more pronounced. Thus, it enlarges the effect of nonlinear analysis, and the results of linear and nonlinear analysis move away from each other. Purely, the higher the fundamental natural frequencies of the system, the further visible the nonlinear frequencies. More valuable point that can be extracted from this figure is that the effect of rising in value of the strain gradient parameter is greater on the boundary condition with lower degrees of freedom. According to the figure, the clamped-clamped boundary condition is affected largely by growing the value of the strain gradient parameter and the incremental trend occurs more rapidly in this less flexible boundary condition.

4.2.3 The effect of magnetic field

Figure 4 provides the effect of the magnetic field on the linear and nonlinear frequencies and a comparison between these two frequency modes by changing the amount of magnetic potential. Based on the data in the figure, it can be realized that increasing the values of the magnetic potential will lead to a rise in the eigenfrequency of the system in

both linear and nonlinear states. In addition, the slope of the increment in the values of the frequencies in the nonlinear case is steeper than the linear one. Physically, it can be deduced that since the positive magnetic potential, in general, the positive magnetic field has a tightening effect on materials due to the contraction, the large amounts of positive magnetic potential can make greater natural frequencies and provide clearly the nonlinear frequency impact. Hence, the results of linear and nonlinear frequencies move away from each other. To conclude the discussion on the effect of magnetic potential, the boundary conditions can be considered through which several boundary conditions are studied. As can be observed from the figure, the incremental slope of the nonlinear frequency values resulting from the increase in the magnetic potential at all boundary conditions will be steeper. Therefore, it can be concluded that in high values of magnetic potential and in general in strong magnetic fields, the difference between the nonlinear frequencies and the linear ones is further notable.

4.2.4 The effect of slenderness ratio

Figure 5 displays a consideration of the effect of length-to-diameter ratio (slenderness ratio) for the problem. It is worthy to note that the difference between nonlinear and linear cases increments by enlarging the length of the beam. It can be said that when the beam's length is long, the effect of nonlinear analysis is considerable. This can display the role of nonlinear analysis in vibrating behavior and emphasize on using this model of study.

4.2.5 The effect of axial inertia

In this work, we implemented the axial inertia effect in the formulation of eigenfrequencies contrarily to what has been usually accomplished. To demonstrate this effect, Figure 6 is plotted. This effect has been ignored in many studies performed on nonlinear vibrations of small or macro scale structures. As seen by Figure 6, while the effect is included, the nonlinear frequencies decrease. One can see the more pronounced discrepancy for lower values of slenderness ratio where the axial inertia causes appreciable reductions into the frequencies. This conclusion corresponds to the foregoing numerical data [106].

To make the effect of axial inertia rather obvious, some tabular results are presented by Table 6 in which assorted boundary conditions are inspected. As seen by the table, the presence of axial inertia is more prominent for tubes with fully fixed ends. All in all, how we can terminate this discussion is that the axial inertia can be an effective factor in nonlinear vibration studies of macro/nano-structures.

5. Conclusions

This study analyzed nonlinear frequencies for a nanotube concerning the Euler-Bernoulli motion field. To accomplish the nanoscale size effect, the motion equations were shifted into NSGT relations. The relations governing the problem which are the nonlinear partial differential equations, were obtained by which the nonlinear vibrational equations of the PF-NT were computed. It was then converted to nonlinear algebraic equations by the Rayleigh-Ritz method. Free vibrations have been investigated in two cases, linear and nonlinear, for some kinds of boundary conditions: simply supported –simply supported, clamped–clamped, and clamped–simply supported. The results were compared with those of Navier's solution and the parametric analysis of the results was presented. The most superior shortened points harvested by our work can be implied as follows which can aid the designers in the MEMS/NEMS industries:

* Whenever the fundamental natural frequencies of a nanotube are enough big, the nonlinear frequencies will be more vital. In this category, the less flexible boundary conditions, the higher values of strain gradient, the longer nanotube, and a stronger positive magnetic field bring about greater fundamental natural frequencies.

* The shorter the length of the nanotube, the larger the effect of axial inertia.

Conflict of Interest Statement

The authors declare that they have no known competing financial interests or personal relationships that could have appeared to influence the work reported in this paper.

References

[1] W. Fahrner, Nanotechnology and Nanoelectronics, Springer, (2005). DOI: 10.1007/b137771

[2] A. F. Kabychenkov, F. V. Lisovskii, Flexomagnetic and flexoantiferromagnetic effects in centrosymmetric antiferromagnetic materials, Technical Physics, 64 (2019) 980-983.

[3] E. A. Eliseev, A. N. Morozovska, M. D. Glinchuk, R. Blinc, Spontaneous flexoelectric/flexomagnetic effect in nanoferroics, Physical Review B, 79 (2009) 165433.

[4] P. Lukashev, R. F. Sabirianov, Flexomagnetic effect in frustrated triangular magnetic structures, Physical Review B, 82 (2010) 094417.

[5] L.-L. Ke, Y.-S. Wang, Free vibration of size-dependent magneto-electro-elastic nanobeams based on the nonlocal theory, Physica E: Low-dimensional Systems and Nanostructures, 63 (2014) 52-61.

[6] T.-P. Chang, Nonlinear free vibration analysis of nanobeams under magnetic field based on nonlocal elasticity theory, Journal of Vibroengineering, 18 (2016) 1912-1919.

[7] M. Baghani, M. Mohammadi, A. Farajpour, Dynamic and Stability Analysis of the Rotating Nanobeam in a Nonuniform Magnetic Field Considering the Surface Energy, International Journal of Applied Mechanics, 8 (2016) 1650048.

[8] F. Ebrahimi, M. R. Barati, Porosity-dependent vibration analysis of piezo-magnetically actuated heterogeneous nanobeams, Mechanical Systems and Signal Processing, 93 (2017) 445-459.

[9] A. M. Zenkour, M. Arefi, N. A. Alshehri, Size-dependent analysis of a sandwich curved nanobeam integrated with piezomagnetic face-sheets, Results in Physics, 7 (2017) 2172-2182.

[10] X.-P. Sun, Y.-.Z. Hong, H.-L. Dai, L. Wang, Nonlinear frequency analysis of buckled nanobeams in the presence of longitudinal magnetic field, Acta Mechanica Solida Sinica, 30 (2017) 465-473.

[11] M. Arefi, A. M. Zenkour, Transient sinusoidal shear deformation formulation of a size-dependent three-layer piezo-magnetic curved nanobeam, Acta Mechanica, 228 (2017) 3657-3674.

[12] H. Liu, H. Liu, J. Yang, Vibration of FG magneto-electro-viscoelastic porous nanobeams on visco-Pasternak foundation, Composites Part B: Engineering, 155 (2018) 244-256.

[13] M. Arefi, A. H. Soltan Arani, Higher order shear deformation bending results of a magnetoelectrothermoelastic functionally graded nanobeam in thermal, mechanical, electrical, and magnetic environments, Mechanics Based Design of Structures and Machines, an International Journal, 46 (2018) 669-692.

[14] B. Alibeigi, Y. T. Beni, On the size-dependent magneto/electromechanical buckling of nanobeams, The European Physical Journal Plus, 133 (2018) 398.

[15] A. Azar, M. Ben Said, L. Azrar, A. A. Aljinaidi, Dynamic instability analysis of magneto-electro-elastic beams with uncertain parameters under static and parametric electric and magnetic fields, Composite Structures, 226 (2019) 111185.

[16] Y.-X. Zhen, S.-L. Wen, Y. Tang, Free vibration analysis of viscoelastic nanotubes under longitudinal magnetic field based on nonlocal strain gradient Timoshenko beam model, Physica E: Low-dimensional Systems and Nanostructures, 105 (2019) 116-124.

[17] M. Malikan, V. B. Nguyen, Buckling analysis of piezo-magnetoelectric nanoplates in hygrothermal environment based on a novel one variable plate theory combining with higher-order nonlocal strain gradient theory, Physica E: Low-dimensional Systems and Nanostructures, 102 (2018) 8-28.

[18] S. S. Mirjavadi, M. Forsat, M. Nikookar, M. Reza Barati, AMS Hamouda, Nonlinear forced vibrations of sandwich smart nanobeams with two-phase piezo-magnetic face sheets, The European Physical Journal Plus, 134 (2019) 508.

[19] S. S. Mirjavadi, M. Forsat, M. Nikookar, M. Reza Barati, AMS Hamouda, Post-buckling analysis of piezo-magnetic nanobeams with geometrical imperfection and different piezoelectric contents, Microsystem Technologies, 25 (2019) 3477-3488.

[20] M. Ghane, A. Reza Saidi, R. Bahaadini, Vibration of fluid-conveying nanotubes subjected to magnetic field based on the thin-walled Timoshenko beam theory, Applied Mathematical Modelling, 80 (2020) 65-83.

[21] S. Sidhardh, M. C. Ray, Flexomagnetic response of nanostructures, Journal of Applied Physics, 124 (2018) 244101.

[22] N. Zhang, Sh. Zheng, D. Chen, Size-dependent static bending of flexomagnetic nanobeams, Journal of Applied Physics, 126 (2019) 223901.

[23] M. Malikan, V. A. Eremeyev, Free Vibration of Flexomagnetic Nanostructured Tubes Based on Stress-driven Nonlocal Elasticity, Springer Nature, Analysis of Shells, Plates, and Beams, Advanced Structured Materials, 134 (2020). https://doi.org/10.1007/978-3-030-47491-1_12

[24] R. Ansari, M. Faraji Oskouie, R. Gholami, Size-dependent geometrically nonlinear free vibration analysis of fractional viscoelastic nanobeams based on the nonlocal elasticity theory, Physica E: Low-dimensional Systems and Nanostructures, 75 (2016) 266-271.

[25] M. Faraji Oskouie, R. Ansari, F. Sadeghi, Nonlinear vibration analysis of fractional viscoelastic Euler–Bernoulli nanobeams based on the surface stress theory, Acta Mechanica Solida Sinica, 30 (2017) 416–424.

[26] J. Wang, H. Shen, Nonlinear vibrations of axially moving simply supported viscoelastic nanobeams based on nonlocal strain gradient theory, Journal of Physics: Condensed Matter, 31 (2019) 485403.

[27] D. D. Nguyen, D. Q. Vu, D. N. Pham, M. C. Trinh, Nonlinear Dynamic Response of Functionally Graded Porous Plates on Elastic Foundation Subjected to Thermal and Mechanical Loads, Journal of Applied and Computational Mechanics, 4 (2018) 245-259.

[28] Hanif S. Hoseini, Dewey H. Hodges, Nonlinear flutter and limit-cycle oscillations of damaged highly flexible composite wings, Nonlinear Dynamics, 97 (2019) 247–268.

[29] G. Ferrari, P. Balasubramanian, S. Le Guisquet, L. Piccagli, K. Karazis, B. Painter, M. Amabili, Non-linear vibrations of nuclear fuel rods, Nuclear Engineering and Design, 338 (2018) 269–283.

[30] V. A. Eremeyev, W. Pietraszkiewicz, The nonlinear theory of elastic shells with phase transitions, Journal of Elasticity, 74 (2004) 67-86.

[31] H. M. Sedighi, A. Koochi, F. Daneshmand, M. Abadyan, Non-linear dynamic instability of a double-sided nano-bridge considering centrifugal force and rarefied gas flow, International Journal of Non-Linear Mechanics, 77 (2015) 96-106.

[32] H. M. Sedighi, K. Heidari Shirazi, A. Noghrehabadi, A. Yildirim, Asymptotic investigation of buckled beam nonlinear vibration, Iranian Journal of Science and Technology: Transactions of Mechanical Engineering, 36 (2012) 107-116.

[33] H. M. Sedighi, F. Daneshmand, Nonlinear transversely vibrating beams by the homotopy perturbation method with an auxiliary term, Journal of Applied and Computational Mechanics, 1 (2014) 1-9.

[34] Y. Li, M. Li, Dynamic analysis of rotating double-tapered cantilever Timoshenko nano-beam using the nonlocal strain gradient theory, Mathematical Methods in the Applied Sciences, (2020). https://doi.org/10.1002/mma.6616

[35] B. Safaei, N. A. Ahmed, A. M. Fattahi, Free vibration analysis of polyethylene/CNT plates, The European Physical Journal Plus, 134 (2019) 271.

[36] J. Guo, D. Xu, W. Qiu, A finite difference scheme for the nonlinear time-fractional partial integro-differential equation, Mathematical Methods in the Applied Sciences, (2020). https://doi.org/10.1002/mma.6128

[37] R. Rezzag Bara, S. Nicaise, I. Merabet, Finite element approximation of a prestressed shell model, Mathematical Methods in the Applied Sciences, (2020). https://doi.org/10.1002/mma.6196

[38] B. Safaei, The effect of embedding a porous core on the free vibration behavior of laminated composite plates, Steel and Composite Structures, 35 (2020) 659-670.

[39] B. Safaei, R. Moradi-Dastjerdi, K. Behdinan, Z. Qin, F. Chu, Thermoelastic behavior of sandwich plates with porous polymeric core and CNT clusters/polymer nanocomposite layers, Composite Structures, 226 (2019) 111209.

[40] M. E. Golmakani, M. N. Sadraee Far, M. Moravej, Dynamic relaxation method for nonlinear buckling analysis of moderately thick FG cylindrical panels with various boundary conditions, Journal of Mechanical Science and Technology, 30 (2016) 5565–5575.

[41] H. M. Sedighi, K. Heidari Shirazi, Using homotopy analysis method to determine profile for disk cam by means of optimization of dissipated energy, International Review of Mechanical Engineering (I.RE.M.E.), Vol. 05, 2011, n. 5

[42] A. Johan, W. Ari Adi, F. Suryani Arsyad, D. Setiabudidaya, Analysis crystal structure of magnetic materials $Co_{1-x}Zn_xFe_2O_4$, Journal of Physics: Conference Series, 1282 (2019) 012032.

[43] X. Song, S.-R. Li, Thermal buckling and post-buckling of pinned–fixed Euler–Bernoulli beams on an elastic foundation, Mechanics Research Communications, 34 (2007) 164–171.

[44] J. N. Reddy, Nonlocal nonlinear formulations for bending of classical and shear deformation theories of beams and plates, International Journal of Engineering Science, 48 (2010) 1507-1518.

[45] M. Moory-Shirbani, H. M. Sedighi, H. M. Ouakad, F. Najar, Experimental and mathematical analysis of a piezoelectrically actuated multilayered imperfect microbeam subjected to applied electric potential, Composite Structures, 184 (2018) 950-960.

[46] H. M. Ouakad, H. M. Sedighi, Static response and free vibration of MEMS arches assuming out-of-plane actuation pattern, International Journal of Non-Linear Mechanics, 110 (2019) 44-57.

[47] R. Ansari, S. Ajori, B. Arash, Vibrations of single- and double-walled carbon nanotubes with layerwise boundary conditions: A molecular dynamics study, Current Applied Physics, 12 (2012) 707-711.

[48] S. Seifoori, F. Abbaspour, E. Zamani, Molecular dynamics simulation of impact behavior in multi-walled carbon nanotubes, Superlattices and Microstructures, 14 (2020) 106447.

[49] F. Ebrahimi, A. Dabbagh, Vibration analysis of multi-scale hybrid nanocomposite plates based on a Halpin-Tsai homogenization model, Composites Part B: Engineering, 173 (2019) 106955.

[50] F. Ebrahimi, A. Dabbagh, An analytical solution for static stability of multi-scale hybrid nanocomposite plates, Engineering with Computers (2019). https://doi.org/10.1007/s00366-019-00840-y

[51] H. Altenbach, V. A. Eremeyev, On the Continuum Mechanics Approach in Modeling Nanosized Structural Elements, New Frontiers of Nanoparticles and Nanocomposite Materials. Advanced Structured Materials, 4 (2012). https://doi.org/10.1007/8611_2012_67

[52] H. Zeighampour, Y. Tadi Beni, Size-dependent vibration of fluid-conveying double-walled carbon nanotubes using couple stress shell theory, Physica E: Low-dimensional Systems and Nanostructures, 61 (2014) 28-39.

[53] B. Akgöz, Ö. Civalek, Free vibration analysis for single-layered graphene sheets in an elastic matrix via modified couple stress theory, Materials and Design 42 (2012) 164-171.

[54] M. Malikan, Electro-mechanical shear buckling of piezoelectric nanoplate using modified couple stress theory based on simplified first order shear deformation theory, Applied Mathematical Modelling, 48 (2017) 196-207.

[55] A. Skrzat, V. A. Eremeyev, On the effective properties of foams in the framework of the couple stress theory, Continuum Mechanics and Thermodynamics (2020). https://doi.org/10.1007/s00161-020-00880-6

[56] H. M. Sedighi, A. Bozorgmehri, Dynamic instability analysis of doubly clamped cylindrical nanowires in the presence of Casimir attraction and surface effects using modified couple stress theory, Acta Mechanica, 227 (2016) 1575–1591.

[57] Y. Yuan, K. Zhao, Y. Han, S. Sahmani, B. Safaei, Nonlinear oscillations of composite conical microshells with in-plane heterogeneity based upon a couple stress-based shell model, Thin-Walled Structures, 154 (2020) 106857.

[58] A. M. Fattahi, B. Safaei, N. A. Ahmed, A comparison for the non-classical plate model based on axial buckling of single-layered graphene sheets, The European Physical Journal Plus, 134 (2019) 555.

[59] B. Safaei, F. Hamed Khoda, A. M. Fattahi, Non-classical plate model for single-layered graphene sheet for axial buckling, Advances in Nano Research, 7 (2019) 265-275.

[60] N. Radić, D. Jeremić, S. Trifković, M. Milutinović, Buckling analysis of double-orthotropic nanoplates embedded in Pasternak elastic medium using nonlocal elasticity theory, Composites Part B: Engineering, 61 (2014) 162-171.

[61] M. Aydogdu, A general nonlocal beam theory: Its application to nanobeam bending, buckling and vibration, Physica E: Low-dimensional Systems and Nanostructures, 41 (2009) 1651-1655.

[62] J. N. Reddy, S. El-Borgi, Eringen's nonlocal theories of beams accounting for moderate rotations, International Journal of Engineering Science, 82 (2014) 159-177.

[63] M. S. Atanasov, V. Stojanović, Nonlocal forced vibrations of rotating cantilever nano-beams, European Journal of Mechanics - A/Solids, 79 (2020) 103850.

[64] S. A. M. Ghannadpour, Ritz Method Application to Bending, Buckling and Vibration Analyses of Timoshenko Beams via Nonlocal Elasticity, Journal of Applied and Computational Mechanics, 4 (2018) 16-26.

[65] R. D. Mindlin, Second gradient of train and surface-tension in linear elasticity, International Journal of Solids and Structures, 1 (1965) 417-438.

[66] R. D. Mindlin, N. N. Eshel, On first strain-gradient theories in linear elasticity, International Journal of Solids and Structures, 4 (1968) 109-124.

[67] B. Akgöz, Ö. Civalek, Longitudinal vibration analysis for microbars based on strain gradient elasticity theory, Journal of Vibration and Control, 20 (2014) 606-616.

[68] H. M. Sedighi, Size-dependent dynamic pull-in instability of vibrating electrically actuated microbeams based on the strain gradient elasticity theory, Acta Astronautica, 95 (2014) 111-123.

[69] C. W. Lim, G. Zhang, J. N. Reddy, A Higher-order nonlocal elasticity and strain gradient theory and Its Applications in wave propagation, Journal of the Mechanics and Physics of Solids, 78 (2015) 298-313.

[70] G. Romano, R. Barretta, Nonlocal elasticity in nanobeams: the stress-driven integral model, International Journal of Engineering Science, 115 (2017) 14-27.

[71] R. Barretta, F. Fabbrocino, R. Luciano, et al. Closed-form solutions in stress-driven two-phase integral elasticity for bending of functionally graded nano-beams, Physica E, 97 (2018) 13-30.

[72] C. C. Koutsoumaris, K.G. Eptaimeros, A research into bi-Helmholtz type of nonlocal elasticity and a direct approach to Eringen's nonlocal integral model in a finite body, Acta Mechanica, 229 (2018) 3629-3649.

[73] M. Lazar, G. A. Maugin, E. C. Aifantis, On a theory of nonlocal elasticity of bi-Helmholtz type and some applications, International Journal of Solids and Structures, 43 (2006) 1404-1421.

[74] M. Şimşek, Some closed-form solutions for static, buckling, free and forced vibration of functionally graded (FG) nanobeams using nonlocal strain gradient theory, Composite Structures, 224 (2019) 111041.

[75] B. Karami, M. Janghorban, On the dynamics of porous nanotubes with variable material properties and variable thickness, International Journal of Engineering Science, 136 (2019) 53-66.

[76] M. Malikan, M. Krasheninnikov, V. A. Eremeyev, Torsional stability capacity of a nano-composite shell based on a nonlocal strain gradient shell model under a three-dimensional magnetic field, International Journal of Engineering Science, 148 (2020) 103210.

[77] S. Sahmani, B. Safaei, Nonlinear free vibrations of bi-directional functionally graded micro/nano-beams including nonlocal stress and microstructural strain gradient size effects, Thin-Walled Structures, 140 (2019) 342-356.

[78] H. Tang, L. Li, Y. Hu, W. Meng, K. Duan, Vibration of nonlocal strain gradient beams incorporating Poisson's ratio and thickness effects, Thin-Walled Structures, 137 (2019) 377-391.

[79] B. Karami, M. Janghorban, T. Rabczuk, Dynamics of two-dimensional functionally graded tapered Timoshenko nanobeam in thermal environment using nonlocal strain gradient theory, Composites Part B: Engineering, 182 (2020) 107622.

[80] F. Ebrahimi, M. R. Barati, Hygrothermal effects on vibration characteristics of viscoelastic FG nanobeams based on nonlocal strain gradient theory, Composite Structures, 159 (2017) 433-444.

[81] P. R. Saffari, M. Fakhraie, M. A. Roudbari, Nonlinear vibration of fluid conveying cantilever nanotube resting on visco-pasternak foundation using non-local strain gradient theory, Micro & Nano Letters, 15 (2020) 181.

[82] M. H. Ghayesh, A. Farajpour, Nonlinear coupled mechanics of nanotubes incorporating both nonlocal and strain gradient effects, Mechanics of Advanced Materials and Structures, 27 (2020) 373-382.

[83] M. Malikan, R. Dimitri, F. Tornabene, Transient response of oscillated carbon nanotubes with an internal and external damping, Composites Part B: Engineering, 158 (2019) 198-205.

[84] M. Malikan, V. A. Eremeyev, On the dynamics of a visco-piezo-flexoelectric nanobeam, Symmetry, 12 (2020) 643. doi: 10.3390/sym12040643

[85] J. Zare, A. Shateri, Y. Tadi Beni, A. Ahmadi, Vibration analysis of shell-like curved carbon nanotubes using nonlocal strain gradient theory, Mathematical Methods in the Applied Sciences, (2020). https://doi.org/10.1002/mma.6599

[86] R. Ansari, S. Sahmani, B. Arash, Nonlocal plate model for free vibrations of single-layered graphene sheets, Physics Letters A, 375 (2010) 53-62.

[87] M. Akbarzadeh Khorshidi, The material length scale parameter used in couple stress theories is not a material constant, International Journal of Engineering Science, 133 (2018) 15-25.

[88] S. K. Jena, S. Chakraverty, F. Tornabene, Vibration characteristics of nanobeam with exponentially varying flexural rigidity resting on linearly varying elastic foundation using differential quadrature method, Materials Research Express, 6 (2019) 085051.

[89] R. Dimitri, F. Tornabene, J. N. Reddy, Numerical study of the mixed-mode behavior of generally-shaped composite interfaces, Composite Structures, 237 (2020) 111935.

[90] R. Ansari, S. Sahmani, H. Rouhi, Rayleigh–Ritz axial buckling analysis of single-walled carbon nanotubes with different boundary conditions, Physics Letters, A 375 (2011) 1255–1263.

[91] M. Teifouet, A. Robinson, S. Adali, Buckling of nonuniform and axially functionally graded nonlocal Timoshenko nanobeams on Winkler-Pasternak foundation, Composite Structures, 206 (2018) 95-103.

[92] Y. Wang, D. Cao, J. Peng, H. Cheng, H. Lin, W. Huang, Nonlinear random responses and fatigue prediction of elastically restrained laminated composite panels in thermo-acoustic environments, Composite Structures, 229 (2019) 111391.

[93] M. Malikan, V. A. Eremeyev, Post-critical buckling of truncated conical carbon nanotubes considering surface effects embedding in a nonlinear Winkler substrate using the Rayleigh-Ritz method, Materials Research Express, 7 (2020) 025005.

[94] S. K. Jena, S. Chakraverty, F. Tornabene, Buckling Behavior of Nanobeams Placed in Electromagnetic Field Using Shifted Chebyshev Polynomials-Based Rayleigh-Ritz Method, Nanomaterials, 9 (2019) 1326.

[95] R. Barretta, F. Marotti de Sciarra, Constitutive boundary conditions for nonlocal strain gradient elastic nano-beams, International Journal of Engineering Science, 130 (2018) 187–198.

[96] R. Barretta, F. Marotti de Sciarra, Variational nonlocal gradient elasticity for nano-beams, International Journal of Engineering Science, 143 (2018) 73–91.

[97] F. Marotti de Sciarra, R. Barretta, A new nonlocal bending model for Euler–Bernoulli nanobeams, Mechanics Research Communications, 62 (2014) 25–30.

[98] G. Romano, R. Barretta, M. Diaco, F. Marotti de Sciarra, Constitutive boundary conditions and paradoxes in nonlocal elastic nanobeams, International Journal of Mechanical Sciences, 121 (2017) 151-156.

[99] L. Lu, X. Guo, J. Zhao, Size-dependent vibration analysis of nanobeams based on the nonlocal strain gradient theory, International Journal of Engineering Science, 116 (2017) 12–24.

[100] S. K. Jena, S. Chakraverty, M. Malikan, Application of shifted Chebyshev polynomial-based Rayleigh–Ritz method and Navier's technique for vibration analysis of a functionally graded porous beam embedded in Kerr foundation, Engineering with Computers (2020). https://doi.org/10.1007/s00366-020-01018-7

[101] T. Pirbodaghi, M.T. Ahmadian, M. Fesanghary, On the homotopy analysis method for non-linear vibration of beams, Mechanics Research Communication, 36 (2009) 143–148.

[102] H. Rafieipour, S. M. Tabatabaei, M. Abbaspour, A novel approximate analytical method for nonlinear vibration analysis of Euler–Bernoulli and Rayleigh beams on the nonlinear elastic foundation, Arabian Journal for Science and Engineering, 39 (2014) 3279–3287.

[103] A. Mirzabeigy, R. Madoliat, Large amplitude free vibration of axially loaded beams resting on variable elastic foundation, Alexandria Engineering Journal, 55 (2016) 1107–1114.

[104] W. H. Duan, C. M. Wang, Exact solutions for axisymmetric bending of micro/nanoscale circular plates based on nonlocal plate theory, Nanotechnology, 18 (2007) 385704.

[105] W. H. Duan, C. M. Wang, Y. Y. Zhang, Calibration of nonlocal scaling effect parameter for free vibration of carbon nanotubes by molecular dynamics, Journal of Applied Physics, 101 (2007) 24305.

[106] A. N. Kounadis, D. Sophianopoulos, The effect of axial inertia on the bending eigenfrequencies of a Timoshenko two-bar frame, Earthquake Engineering and Structural Dynamics, 14 (1986) 429-437.

Table 1. Conditions at both ends based on notations

Conditions	$\eta(x=0)$	$\xi(x=L)$
SS	1	1
CS	2	1
CC	2	2

Table 2. Constitutive boundary conditions

Conditions	Nonlocal strain gradient conditions at (0, L)	Local conditions ($l=\mu=0$) at (0, L)
S	w=0 $M=-\left(1+l^2\frac{d^2}{dx^2}\right)M_{cl}+\mu\frac{d}{dx}\left(N_{cl}\frac{dw}{dx}\right)=0$ $M_h=\frac{dM_{cl}}{dx}=0$ $T_{xxz}=-g_{31}h\frac{d^2w}{dx^2}+f_{31}\psi=0$	w=0 $M_{cl}=0$ $T_{xxz}=0$
C	w=0 w'=0 $M\neq 0$ $M_h\neq 0$ $T_{xxz}=0$	w=0 w'=0 $M_{cl}\neq 0$ $T_{xxz}=0$

* Sub-indexes (h and cl) are nonlocal and local phases, respectively.

Table 3. Nondimensional natural frequencies of a square nanobeam (First mode, L=10 nm, h=1 nm, ν =0.3, E=1TPa, ρ =2.7kg/dm^3)

L/h	μ	ω_L

		EBT, Navier [99]	EBT, Navier [Present]	EBT, Rayleigh-Ritz, [Present]
5	0	9.7112	9.7112	9.7112
	1	9.2647	9.2647	9.2647
	2	8.8747	8.8747	8.8747
	3	8.5301	8.5301	8.5301
	4	8.2228	8.2228	8.2228
10	0	9.8293	9.8293	9.8293
	1	9.3774	9.3774	9.3774
	2	8.9826	8.9826	8.9826
	3	8.6338	8.6338	8.6338
	4	8.3228	8.3228	8.3228
20	0	9.8595	9.8595	9.8595
	1	9.4062	9.4062	9.4062
	2	9.0102	9.0102	9.0102
	3	8.6604	8.6604	8.6604
	4	8.3483	8.3483	8.3483

Table 4. Ratio of nonlinear to linear cases of frequency for a square macro beam (First mode).

ω_{NL}/ω_{L}			
Present	[101]	[102]	[103]
1.0874	1.0897	1.0892	1.0892

Table 5. Magneto-mechanical properties of an assumed piezo-flexomagnetic nanotube (PF-NT)

$CoFe_2O_4$
C_{11}=286e9 N/m^2
f_{31}=10^{-10} N/Ampere
q_{31}=580.3 N/Ampere.m
a_{33}=1.57×10^{-4} N/Ampere^2
L=10d, d=1 nm, h=0.34 nm

Table 6. Slenderness ratio vs. axial inertia effect in the nonlinear study of the PF-NT based on several boundary conditions (Ψ=1 *mA*, *l*=1 *nm*, e_0a=0.5 *nm*)

Axial inertia	*L/d*	CC	CS	SS
Presence	5	41.4830	28.1964	16.8231
	10	34.3034	27.5697	18.4081
	20	35.4480	31.4843	22.9379

	30	40.6439	37.1471	28.3744
	40	47.3009	43.7931	34.4555
	5	45.2122	31.0591	18.0210
	10	35.1884	28.3695	18.7697
Absence	20	35.6849	31.7207	23.0533
	30	40.7655	37.2719	28.4381
	40	47.3806	43.8760	34.4992

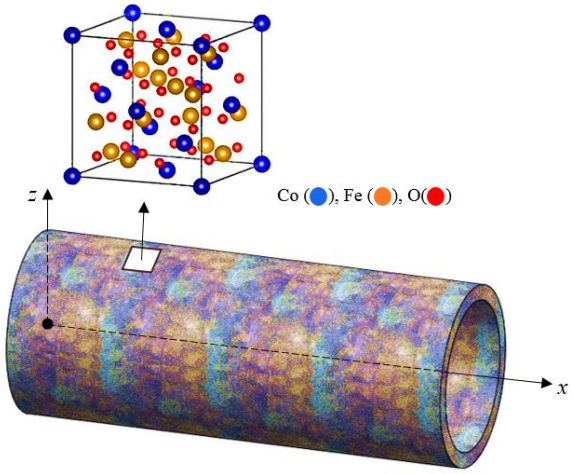

Figure 1. A $CoFe_2O_4$ nanotube

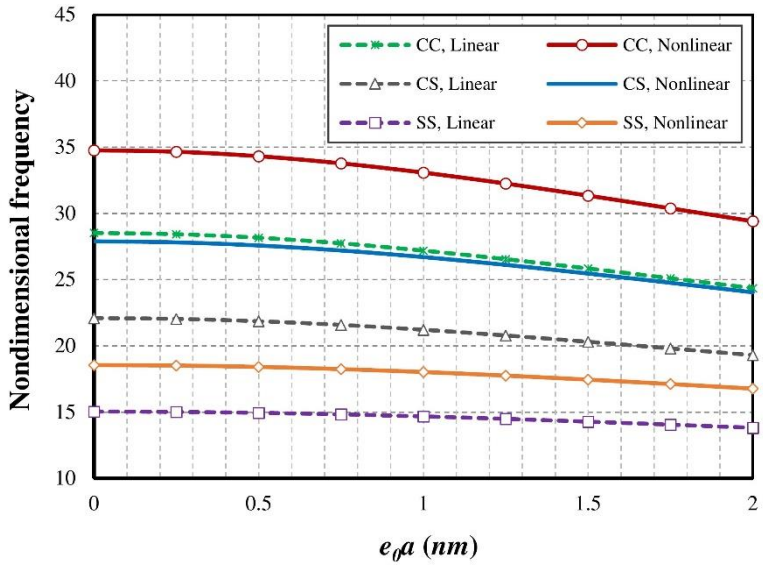

Figure 2. Nonlocal parameter vs. different end conditions for the PF-NT (Ψ=1 *mA*, *l*=1 *nm*)

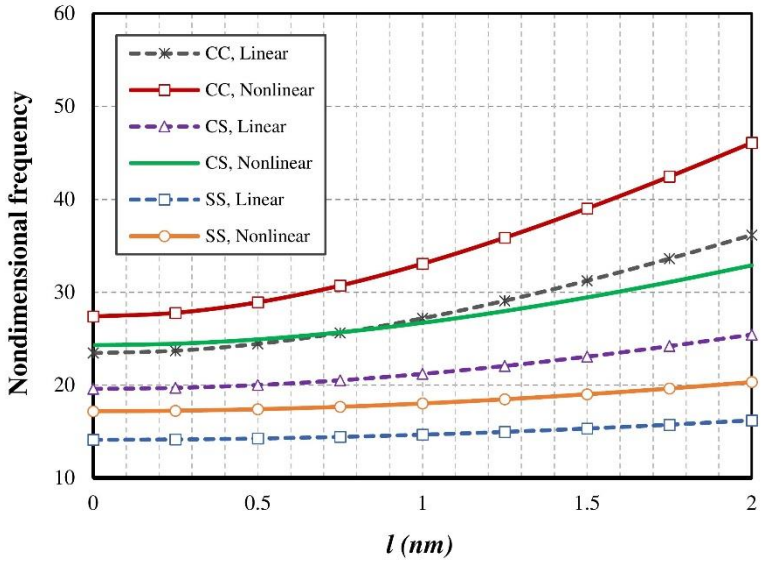

Figure 3. Strain gradient parameter vs. different end conditions for the PF-NT (Ψ=1 *mA*, e_0a=1 nm)

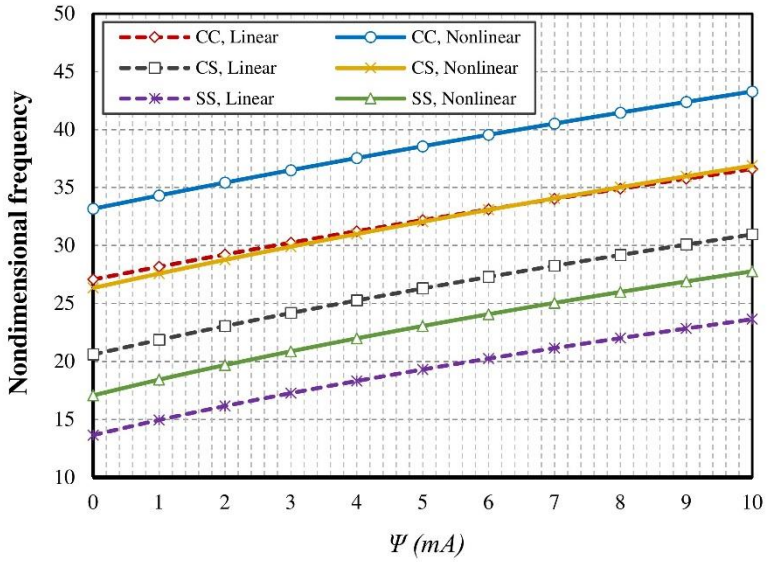

Figure 4. Magnetic potential parameter vs. different end conditions for the PF-NT (l=1 *nm*, e_0a=0.5 *nm*)

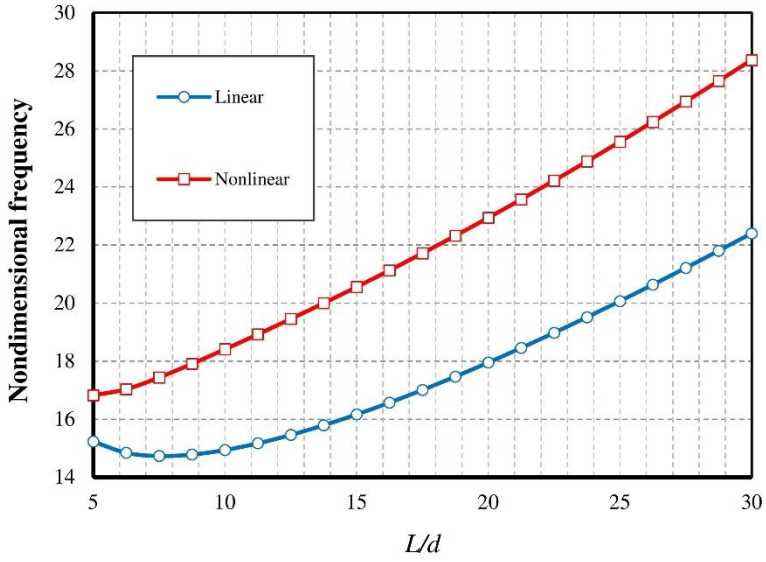

Figure 5. Slenderness ratio vs. linear and nonlinear analyses (Ψ=1 *mA*, *l*=1 *nm*, e_0a=0.5 *nm*, *SS*)

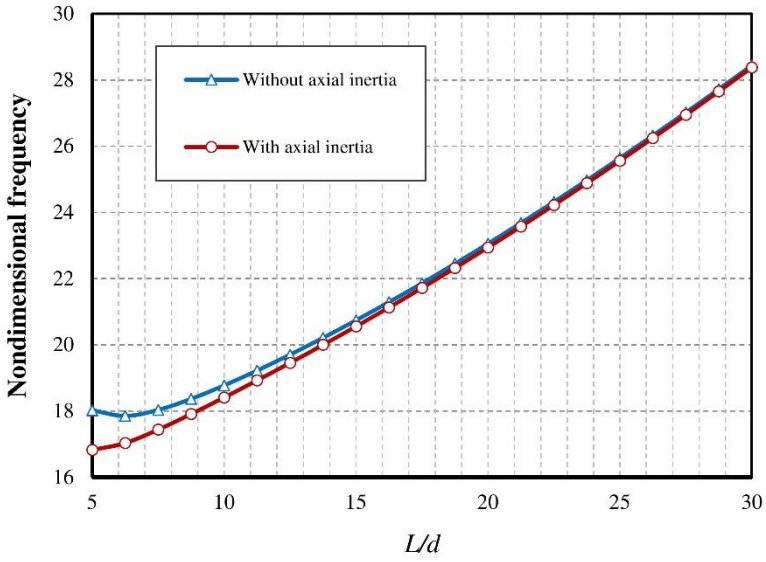

Figure 6. Slenderness ratio vs. the axial inertia effect in the nonlinear case of the PF-NT (Ψ=1 *mA*, *l*=1 *nm*, e_0a=0.5 *nm*, *SS*)